ORIGINAL PAPER

Pectin–cerium (IV) tungstate nanocomposite and its adsorptional activity for removal of methylene blue dye

V. K. Gupta · D. Pathania · P. Singh

Abstract Pectin–cerium (IV) tungstate composite (Pc/CT) has been prepared by sol gel method at room temperature. The composite ion exchanger has been characterized using X-ray diffraction, scanning electron microscopy, energy dispersive X-ray spectroscopy and Fourier infrared spectroscopy. The ion exchange capacity, pH titrations, thermal stability and distribution coefficient of composite ion exchanger were investigated. The Na^+ ions exchange capacity of the Pc/CT has been observed higher (1.4 meq g^{-1}) as compared to its inorganic counterpart (0.8 meq g^{-1}). Pc/CT composite ion exchanger was thermally stable and retained about 60 % of its ion exchange capacity up to 400 °C. The distribution study has inferred more selective the Pc/CT for Zn^{2+} as compared to other metal ions. The adsorption efficiency of Pc/CT was tested for methylene blue removal dye from aqueous phase. The removal of dye followed pseudo-second-order kinetics.

Keywords Pectin–cerium (IV) tungstate ·
Characterization · Methylene blue · Adsorption

V. K. Gupta (✉)
Department of Chemistry, Indian Institute of Technology
Roorkee, Roorkee 247667, India
e-mail: vinodfcy@gmail.com

V. K. Gupta
Dr. R M L Avadh University, Faizabad, UP 224001, India

D. Pathania · P. Singh
School of Chemistry, Shoolini University, Solan 173212,
Himachal Pradesh, India

Introduction

The colored effluent is produced from various industries such as textile, paper, paint, rubber and discharged into water bodies (Ibrahim et al. 2010). The discharged dyes degrade the water quality and are the chief threat to human health due to toxic, mutagenic and carcinogenic nature (Gupta et al. 2012; Huang and Chen 2009). Therefore, colored wastewater cannot be discharged without proper treatment. The organic dyes were not easily removed by conventional wastewater treatment methods due to their complex structure and synthetic origin (Dogan et al. 2004). Thus, the removal of organic dyes from wastewater has been of great interest in the recent years.

Many conventional methods such as coagulation, flocculation, precipitation, membrane separation, solvent extraction and adsorption have been used for the treatment of industrial effluent (Gupta et al. 2007; Zacar and Engil 2004). Among these investigated methods, adsorption is a fast, inexpensive and widely applicable for the removal of dyes due to its simplicity, economic viability and technical feasibility (Pathania and Sharma 2012; Bhattacharyya and Sharma 2005).

It has been observed that many types of adsorbents were effectively used for removing the dyes from aqueous system. Recently, particular attention has been given to bio-polymer-based adsorbents. The bio-adsorbent is low-cost, harmless and abundantly available (Constantin et al. 2013; Yang et al. 2012). A large number of non-conventional bio-adsorbents such as bacterial biomass or bio-polymers have been employed for the remediation of dyes from water body. The lower stability, difficulty in separation from aqueous phase and low recovery after desorption are the major limitations associated with bio-adsorbents (Gupta et al. 2007).

Pectin is a naturally occurring polysaccharide function as an intercellular and intracellular cementing material. It is able to bind with some organic and inorganic substances through molecular interactions. It has been used to prepare matrices for the absorption of desired materials and deliver them in a controlled manner (Shi and Gunasekaran 2008).

Nowadays, hybrid organic–inorganic nanocomposite materials are of enormous importance because of their multifunctionality owing to combination with different compounds incorporated. The composite ion exchangers have been used in environmental remediation because of their selectivity, specificity and wide range of applicability (Khan and Khan 2010; Vatutsina et al. 2007). The attempt has been made by various researches to improve the chemical, mechanical, thermal properties and selectivity of composite ion exchangers for certain heavy metal ions (Islam and Patel 2008; Nabi and Naushad 2008; Bushra et al. 2012; Nabi et al. 2011; Khan and Paquiza 2011). The composite ion exchangers have been used effectively in different fields such as ion selective electrodes, catalysis, hydrometallurgy, bimolecular separations, chromatography and environmental science engineering (Hassan et al. 2001; Nabi et al. 2010; Arrad and Sasson 1989).

The detailed literature survey confirmed that no data are available related to the preparation of pectin–cerium (IV) tungstate composite and its applicability for the removal of organic dye from water system. Therefore, in this work, the synthesized pectin–cerium (IV) tungstate composite has been explored for the degradation of hazardous dye from water system. The ion exchange behavior, ion exchange capacity, pH titrations study and distribution study were explored. Pectin–cerium (IV) tungstate composite was characterized by scanning electron transmission (SEM), transmission electron microscopy (TEM), energy dispersive X-ray (EDX), X-ray diffraction (XRD) and Fourier transform infrared (FTIR).

Materials and method

Reagents

Pectin (Loba Chemia Pvt. Ltd., India), ammonium cerric nitrate (E-Merck, Pvt. Ltd., India), sodium tungstate (Qualigens Pvt. Ltd., India) and sodium molybdate (CDH Pvt. Ltd., India) were the reagents used for synthesis of composite ion exchanger. All other reagents used in this study were also of analytical grade. All experiments were conducted in May 2012 at Solan, Himachal Pradesh.

Instrumentation

A digital pH meter (Elico LI-10, India), Fourier transform infrared (FTIR) spectrophotometer (Perkin Elmer Spectrum-BX USA), X-ray diffractometer (Perkin Elmer Series IICHNS/O 2400), scanning electron microscope (Quanta 250, FEI Make Mode No. D9393), transmission electron microscope (FEI Tecnai F 20), muffle furnace (MSW-275, India) and water bath incubator shaker were used.

Preparation of pectin–cerium (IV) tungstate (Pc/CT)

Pectin-based composite ion exchanger was synthesized using simple and ambient sol gel method as described earlier (Nabi et al. 2011). In this, 0.1 M solution of sodium tungstate was added drop wise with constant stirring to 0.1 M solution of ammonium cerric nitrate at 60 ± 5 °C. After complete addition, the mixture was stirred for 30 min to obtain cerium (IV) tungstate (CT) precipitates. Then, pectin (Pc) gel was prepared in diluted formic acid and added to the solution containing cerium (IV) tungstate with continuous stirring for 4 h. The resultant mixture was kept for 12 h at room temperature with occasional shaking. The supernatant liquid was decanted, and the precipitates of composite exchanger were filtered under suction and washed with double distilled water. The obtained composite material was dried in oven at 50 °C. The dried product was broken into small granules of uniform size and converted into H^+ form, by treating with 1 M HNO_3 for 24 h. Finally, the composite was washed with double distilled water several times to remove excess of acid and dried at 50 °C.

Ion exchange capacity (IEC)

The ion exchange capacity of Pc/CT was determined by method as discussed earlier (Siddiqi and Pathania 2003). In this process, 0.5 g of Pc/CT composite ion exchanger in H^+ form was taken in glass column with internal diameter of 1 cm fitted with glass wool at the bottom; 0.1 M NaCl solution was used as eluant, and flow rate was maintained constant (20 drops per minute). The collected effluent was titrated against a standard alkali solution using indicator. The was calculated using the formula as discussed earlier (Siddiqi and Pathania 2003):

$$IEC = \frac{N \times V}{W} \, mg/g \tag{1}$$

where IEC is ion exchange capacity. N and V (ml) are normality and volume of NaOH, respectively. W (mg) is the weight of composite ion exchanger.

Thermal stability

The thermal stability was determined by heated 0.5 g sample of Pc/CT at different temperatures in muffle furnace for 1 h. After room temperature cooling, sample was weighed and ion exchange capacity was determined by column process as discussed in section "Ion exchange capacity".

pH titration

pH titration studies were performed using batch process. In typical method, 0.5 g of Pc/CT was placed in conical flasks containing equimolar solutions of alkali metal chlorides and their hydroxide in different volume ratios. The pH of solution was observed after every 24 h until equilibrium was attained. The amount of H^+ released from the Pc/CT composite and its ion exchange capacity was determined as per the procedure stated above.

Distribution studies

Distribution coefficient (K_d) of different metals ions was determined in distilled water using typical batch process. In this, 0.5 g of Pc/CT and different metal nitrate solutions (50 ml) were continuously shaken for 24 h in round bottom flaks. The metal ion concentrations were determined by titrating against standard EDTA solution. K_d values (ml/g) were determined using following formula (Siddiqui et al. 2007):

$$K_d = \frac{I - F}{F} \times \frac{V}{M} \qquad (2)$$

where I and F are the initial and final concentrations of metal ion in solution. V and M denote final volume of the solution (ml) and amount of Pc/CT (g), respectively.

Adsorption isotherm

The Langmuir sorption isotherm is applied to equilibrium sorption assuming monolayer sorption onto a surface with a finite number of identical sites.

The Langmuir equation is given by following equation (Langmuir 1916):

$$\frac{1}{q_e} = \frac{1}{q_m} + \frac{1}{K_L q_m C_e} \qquad (3)$$

The separation factor (R_L) determines the feasibility of adsorption process and is given as follows (Foo and Hameed 2012):

$$R_L = \frac{1}{1 + K_L C_o} \qquad (4)$$

where K_L is Langmuir constant (l/mg) related to the affinity of binding sites and the free energy of sorption. q_e is dye concentration at equilibrium onto biosorbent (mg/g). C_e is dye concentration at equilibrium in solution (mg/l). q_m is dye concentration when monolayer forms on biosorbent (mg/g). The Freundlich equation for heterogeneous surface energy systems is represented by Eq. (5) (Foo and Hameed 2012; Nemr et al. 2009).

$$\ln q_e = \ln K_F + \frac{1}{n} \ln C_e \qquad (5)$$

where K_F and n are Freundlich constants, determined from the plot of $\ln q_e$ versus $\ln C_e$. The parameters K_F and $1/n$ related to sorption capacity and the sorption intensity of the system. The magnitude of the term ($1/n$) gives an indication of the favorability of the sorbent/adsorbate systems (Malik 2004).

The linearized Tempkin equation is expressed by following equation (Foo and Hameed 2012; Wang and Qin 2005).

$$q_e = \beta \ln \alpha + \beta \ln C_e \qquad (6)$$

where $\beta = \frac{RT}{b} T$ is the absolute temperature in Kelvin, R is the universal gas constant (8.314 J/mol K), b is the Tempkin constant related to heat of sorption (J/mg). The Tempkin constants α and b are calculated from the slope and intercept of q_e versus $\ln C_e$.

Characterization techniques

Fourier transform infrared absorption spectra (FTIR)

FTIR absorption spectrum of Pc/CT was recorded in the region of 400–4,000 cm^{-1} using KBr disk method. The Pc/CT in H^+ form was thoroughly mixed with KBr and powdered, and disk is formed by applying the pressure.

X-ray diffraction studies

The X-ray diffraction pattern of the Pc/CT was recorded by X-ray diffractometer using CuKα radiation ($\lambda = 1.5418$ Å).

Scanning electron microscopy and energy dispersive X-ray studies

Scanning electron microphotographs of Pc/CT composite ion exchanger were recorded using scanning electron microscope at different magnifications. The elemental composition of the composite material was determined by

2018

Int. J. Environ. Sci. Technol. (2014) 11:2015–2024

energy dispersive X-ray, which is coupled with scanning electron microscopy.

Transmission electron microscopy (TEM)

The transmission electron microscopic images of Pc/CT composite ion exchanger were recorded using Hitachi TEM System. The sample was prepared by dispersing the powdered material in ethanol and sonicated in the sonicator. Then, drops of samples were transferred to copper grids for analysis.

Adsorption experiment

The adsorption experiment was carried out in a batch reactor at 25 ± 0.5 °C (Gupta et al. 2007). Definite amount of methylene blue (MB) dye solution was prepared in double distilled water, and 100 mg of composite ion exchanger in H^+ form was added to form slurry. In adsorption experiments, slurry composed of dye solution and Pc/CT composite ion exchanger suspension were stirred magnetically and placed in dark to establish adsorption–desorption equilibrium. The aliquot (5 ml) of solution was withdrawn at different intervals of time and centrifuged to remove particles of composite form aliquot to analyze dye concentration at 620 nm. The percent degradation of dye was calculated using following formula:

$$\% \, \text{Degradation} = \frac{C_e - C_t}{C_e} \times 100$$

where C_e and C_t are concentration of dye at equilibrium and at time t

Results and discussion

Characterization

Scanning electron microscopy (SEM) images of pectin–cerium (IV) tungstate composite at different magnifications were shown in Fig. 1. Pc/CT exhibits rough surface with different sized particles to form microsphere. TEM images indicated homogeneous distribution of Pc and CT particles in the composite Fig. 1. The darker portion represents pectin wrapped CT, while white portion corresponds to polymeric pectin backbone.

X-ray diffraction pattern of pectin–cerium (IV) tungstate was shown in Fig. 2a. The presence of low intensity broader peaks of CT indicates semicrystalline nature of composite materials.

EDX analysis of Pc/CT was shown in Fig. 2b. EDX analysis confirmed the presence of carbon, cerium,

tungstate and oxygen as the major elements present in the Pc/CT composite ion exchanger.

FTIR spectrum of Pc/CT (Fig. 2c) shows broad peak at $3,555 \, \text{cm}^{-1}$ attributed to the O–H stretching vibration (Liang et al. 2010). The peaks in the regions $852 \, \text{cm}^{-1}$ may be assigned to $(WO_4)^{2-}$ and metal oxide groups, respectively (Miller and Wilkins 1952). The adsorption peak at $1,738 \, \text{cm}^{-1}$ may be due to C=O stretching of ester. The adsorption band at $1,618 \, \text{cm}^{-1}$ may be due to symmetric and asymmetric vibrations of carboxylic acid in ion form (COO^-). The absorption band at $1,200 \, \text{cm}^{-1}$ may be due to the vibration associated with the skeletal ring of sugar monomers of pectin. The presence of characteristics peaks of pectin and tungstate in the spectra clearly indicated the formation of Pc/CT composite ion exchangers.

Ion exchange capacity

The Na^+ ion exchange capacity of Pc/CT was observed higher ($1.32 \, \text{meq g}^{-1}$) compared to inorganic ion exchanger (0.8 meq/g). The greater ion exchange capacity of composite ion exchanger was due to incorporation of pectin into inorganic counterpart.

pH titration study at equilibrium conditions for Pc/CT with NaOH–NaCl system confirmed the monofunctional nature of composite ion exchanger (Nabi et al. 2011). Pc/CT behaves as strong cation exchanger as indicated by a low pH of the solution when no OH^- ions were added.

The distribution studies showed that Pc/CT composite exchanger was found to be highly selective for Zn^{2+} as compared to other metal ions. The selectivity order of different metal ion in Pc/CT composite exchanger was found in the order of Zn > Cd > Mg > Pb.

The effect of temperature on the ion exchange capacity interfered that the Pc/CT composite ion exchanger was thermally stable and retained the ion exchange capacity of 60 % up to 400 °C.

Adsorptional removal of MB

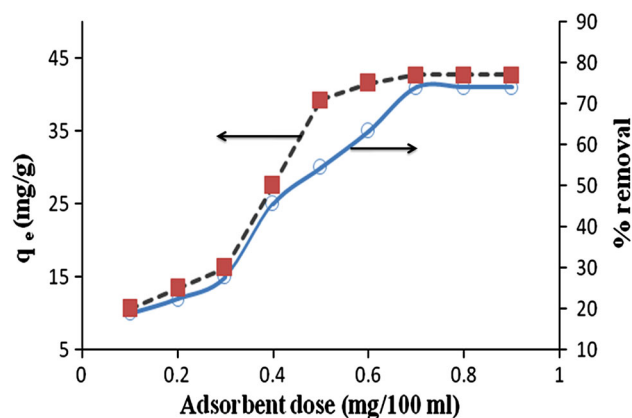#### Effect of adsorbent dose and initial dye concentration

The adsorbent doses were varied from 0.1 to 0.9 g/50 ml. It is evident from Fig. 3 that the MB removal increased sharply with increase in the adsorbent concentration from 0.1 g/100 ml to 0.7 g/100 ml. This was due to availability of more adsorbent sites as well as greater availability of specific surfaces of the adsorbents (Fig. 3). However, no significant changes in removal efficiency were observed beyond 0.5 g/100 ml adsorbent dose. Due to conglomeration of adsorbent particles, there is no increase in effective

Int. J. Environ. Sci. Technol. (2014) 11:2015–2024

2019

Fig. 1 SEM and TEM images of Pc/CT
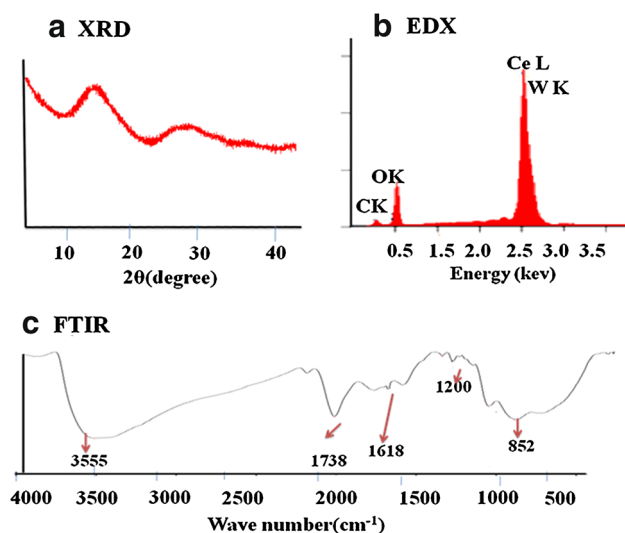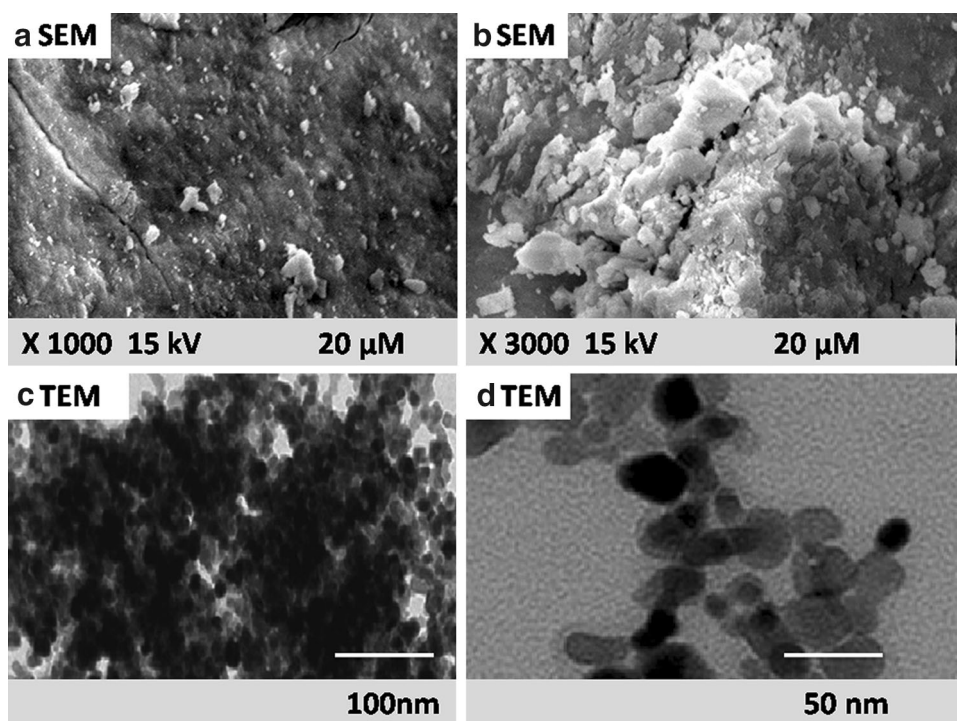
Fig. 2 XRD, EDX and FTIR spectra of Pc/CT

Fig. 3 Effect of Pc/CT dose of methylene blue removal (MB = 50 mg/100 ml, pH = 7, contact time = 60 min, temperature = 25 °C)

surface area of FCBAC (Barka et al. 2011; Zhao et al. 2012a, b). So, 0.7 g/100 ml is considered the optimal dose for FCBAC loading.

The effect of MB concentration on adsorption capacity of Pc/TW was studied in the concentration range of 10–70 mg/100 ml (Fig. 4). Equilibrium adsorption capacity increased with increase in MB concentration from 50 mg/50 ml. Further increase in dye concentration showed no significant changes removal efficiency. This was due to the fact that with increased dye concentration,

the driving force for mass transfer also increases. At low concentration, there will be unoccupied active sites on the adsorbent surface. Above optimal MB concentration, the active sites required for the adsorption of dye will lack (Barka et al. 2011). This retards the overall MB adsorption by activated carbon.

Effect of contact time

The effect of contact time on MB removal is shown in Fig. 5. In 60 min, 75 % of dye removal was observed. The
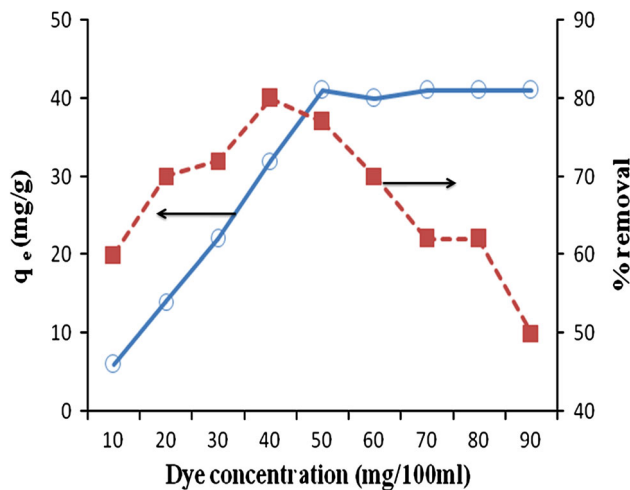
2020

Int. J. Environ. Sci. Technol. (2014) 11:2015–2024

Fig. 4 Effect of MB concentration on adsorption(Pc/CT = 0.4 mg/ 100 ml, pH = 7, contact time = 60 min, temperature = 25 °C.)

Fig. 6 Effect of pH on MB adsorption. (MB = 50 mg/100 ml, Pc/ CT = 0.4 mg/100 ml, contact time, temperature = 25 °C.)
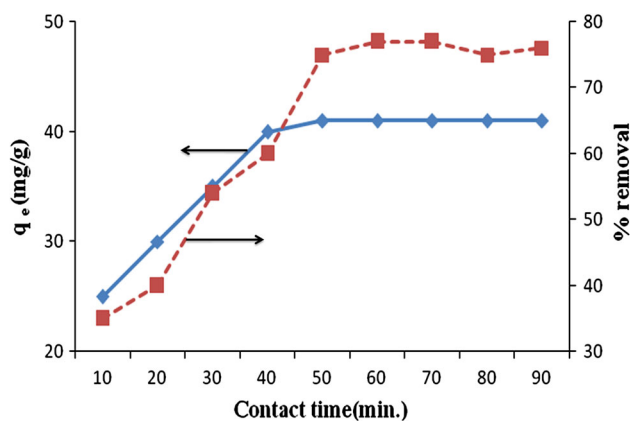

Fig. 5 Effect of contact time on MB adsorption (MB = 50 mg/ 100 ml, Pc/CT = 0.4 mg/100 ml, pH = 7, temperature = 25 °C.)

equilibrium was reached after 80 min. The change in rate of adsorption might be due to fact that initially all the adsorbent sites are vacant and solute concentration gradient is very high. Later, the lower adsorption rate is due to decrease in number of vacant site of adsorbent and dye concentration. The decreased adsorption rate, particularly, toward the end of experiments, indicates the possible monolayer formation of MB on adsorbent surface (Abd et al. 2009). This may be attributed to lack of available active sites required for further uptake after attaining the equilibrium (Liang et al. 2010).

Effect of pH

The pH of a dye solution is an important influencing factor for the adsorption MB onto Pc/TW. Figure 6 shows the
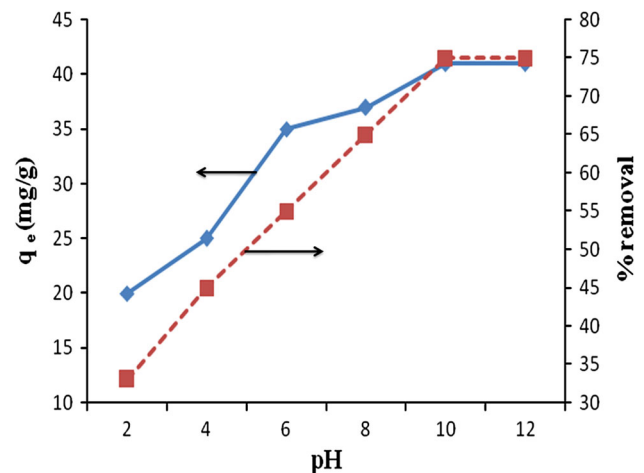
effect of pH on adsorption onto Pc/TW. The maximum MB removal was observed at pH 8. The basic dye gives positively charged ions when dissolved in water. Thus, in acidic medium, positively charged surface of Pc/TW tends to oppose the adsorption of the cationic adsorbate. When pH of dye solution is increased, the surface acquires negative charge, thereby resulting in an increased adsorption of MB due to increase in electrostatic attraction between positively charged dye and negatively charged adsorbent (Abd et al. 2009; Malik 2004).

Adsorption kinetics

The pseudo-first-order rate expression is expressed by following equation:

$$\log(q_e - q_t) = \log q_e - \frac{k_1 t}{2.303} \tag{7}$$

where, q_e and q_t are the amount of dye adsorbed on sorbent at equilibrium and time t (mg/g), k_1 is the first-order rate constant (min^{-1}). A plot of log ($q_e - q_t$) versus t gives a linear relationship, from which the value of k_1 and q_e can be determined from the slope and intercept.

The linearized form of pseudo-second-order rate expression is given as (Pathania and Sharma 2012):

$$\frac{q_t}{dt} = k_2(q_e - q_e)^2 \tag{8}$$
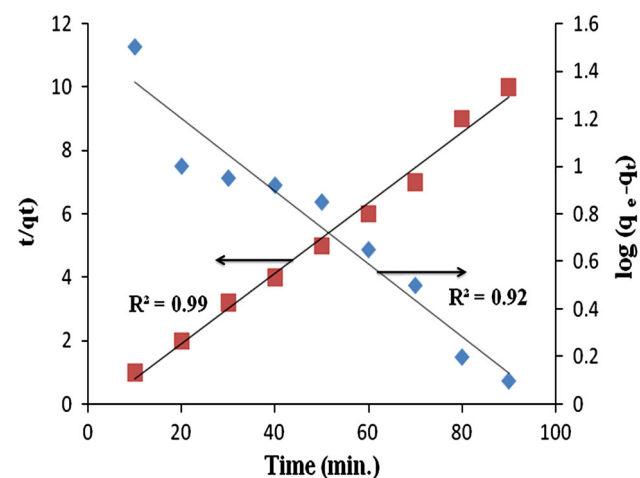
$$\frac{t}{q_t} = \frac{1}{k_2 q_e^2} + \frac{t}{q_e} \tag{9}$$

where q_e is the amount of adsorbate adsorbed per unit mass of sorbent at equilibrium (mg/g), q_t is the amount of adsorbate adsorbed at contact time t (mg/g) and k_2 is the

Table 1 Kinetic and thermodynamic parameters for the sorption of MB onto Pc/CT

Pseudo-first-order model		
k_1 (min^{-1})	q_e (mg/g)	R^2
0.025	40.31	0.92
Pseudo-second-order model		
k_2 (g/mg min)	q_e (mg/g)	R^2
0.00017	41.56	0.99
Intraparticle diffusion model		
k_d (mg/g min)	C (mg/g)	R^2
2.97	3.00	0.99
Thermodynamic parameters		
ΔH^0 (kJ/mol)	ΔS^0 (J/mol K)	ΔG^0 (kJ/mol)
20	66.24	−1.45

Table 2 Various isotherm plots for the adsorption of MB onto Pc/CT

Models	Isotherm constants			
Langmuir	q_m (mg/g)	K_L (l/mg)	R_L	R^2
	41.59	0.04	0.03–0.30	0.99
Freundlich	n	K_F (mg/g)		R^2
	2.12	5.12		0.94
Tempkin	α (l/g)	β (mg/l)	B (J/mg)	R^2
	0.53	9.17	254	0.98

Fig. 7 First-order and second-order kinetic plot for MB adsorption

pseudo-second-order rate constant (g/mg min). A plot of t/q_t versus t gives a linear relationship, from which q_e and k_2 can be determined from the slope and intercept (Bhattacharyya and Sharma 2005).

The data for the adsorption of MB on Pc/TW were applied to pseudo-first- and second-order kinetic models, and the results are presented in Table 1. The correlation coefficient of second-order kinetic model (0.99) is greater than for first-order kinetic model (0.92) (Table 1; Fig. 7). This confirmed that the rate limiting step is chemisorption, involving valence forces through sharing or exchange of electron (Bhattacharyya and Sharma 2005).

The intraparticle diffusion equation is expressed as follows:

$$q_t = K_d t^{1/2} + C \qquad (10)$$

where k_d is the intraparticle diffusion rate constant (mg/g min$^{1/2}$). The data for intraparticle diffusion are given in

Table 1. The linear portion of the plot does not pass through origin. This deviation from the origin was due to the variation of mass transfer in the initial and final stages of adsorption process. This confirms that adsorption of MB on PC/TW was a multistep process involving adsorption on the external surface and diffusion into the interior (Kumar and Kumaran 2005; Gupta et al. 2009, 2010, 2011a, b).

Adsorption isotherm

The adsorption capacity and other parameters were evaluated using Langmuir, Freundlich and Temkin isotherm models. It has been observed that the sorption capacity (q_m) was found to be 41.59 mg/g (Table 2). The high value of correlation coefficient (0.99) signifies the applicability of Langmuir isotherm, which assumes a monolayer coverage and uniform activity distribution on the sorbent surface. In precedent study, R_L values ($0 < R_L < 1$) favor the adsorption of MB onto Pc/CT (Table 2).

Tempkin isotherm was evaluated by Eq. 6. The value of correlation coefficient R^2 obtained from Temkin isotherm was 0.98. Temkin constant b (254 J/mg) is related to heat of sorption indicates physio-chemical nature of sorption process.

The equilibrium data were also fitted to Freundlich equation. The parameters K_F and n indicated the sorption capacity and the sorption intensity of the system. The magnitude of the term (1/n) gives an indication of the favorability of the sorbent/adsorbate systems (Malik 2004). The correlation coefficient value (0.95) is lower than Langmuir and Tempkin values. Therefore, adsorption onto Pc/CT did not follow Freundlich isotherm closely.

Adsorption thermodynamics

Thermodynamic parameters evaluated for MB adsorption onto Pc/CT are the free energy change (ΔG^0), enthalpy change (ΔH^0) and entropy change (ΔS^0). These parameters were calculated using following equation (Gupta et al. 2009, 2010).
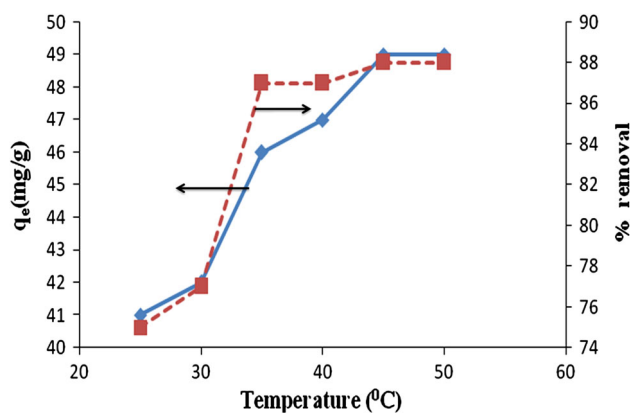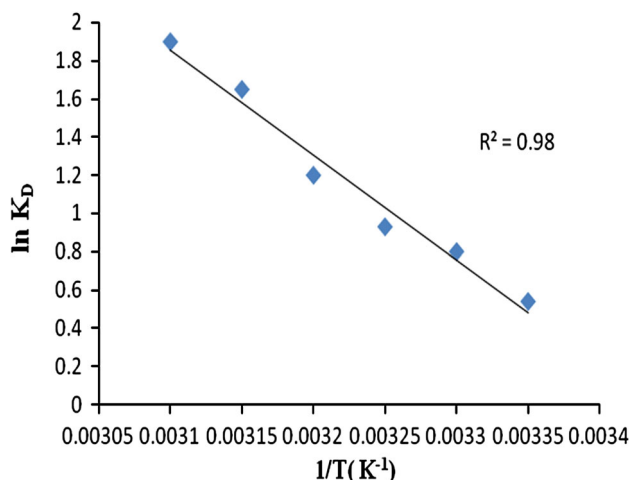
Fig. 8 Effect of temperature onto MB adsorption

Fig. 9 Vant's Hoff plot for MB adsorption onto Pc/CT

$$\Delta G^0 = -2.303RT \log K_D \tag{11}$$

$$K_D = \frac{q_e}{C_e}$$

Also, $\Delta G^0 = \Delta H^0 - T\Delta S^0$ $\tag{12}$

$$\ln K_D = \frac{\Delta S^\circ}{R} - \frac{\Delta H^\circ}{RT} \tag{13}$$

where q_e is MB concentration at equilibrium onto Pc/CT (mg/l), R is universal gas constant (8.314 J/mol K) and C_e is MB concentration at equilibrium in solution (mg/l). The values of ΔH^0 and ΔS^0 were determined from the slope and intercept of the plot of ln K_D versus $1/T$. Gibbs free energy change of sorption (ΔG^0) was calculated using Eq. 11.

Adsorption of dye increased rapidly with increase in temperature from 303 to 343 K (Fig. 8). The increased adsorption capacity of Pc/TW was attributed to the enlargement of pore size and activation of the sorbent

surface with temperature. Further, with rise in temperature increases the mobility of the large dye ions and reduces the swelling effect thus enabling the large dye molecule to penetrate further (Liu and Liu 2008). The results also indicated that adsorption of MB is an endothermic process.

Thermodynamic parameters (ΔH^0, ΔS^0 and ΔG^0) for MB adsorption were evaluated using Eqs. 11–13. The values of ΔH^0 and ΔS^0 were determined from the slope and intercept of the plot of ln K_D versus $1/T$ (Fig. 9). Table 2 shows the thermodynamic parameters for MB adsorption onto FCBAC. The positive value of ΔH^0 (20 kJ/mol) indicates that adsorption of MB onto FCBAC is endothermic reaction. The calculated value of ΔG^0 (−1.45 kJ/mol) indicates spontaneous nature of adsorption process. Further the positive value of entropy change, ΔS^0 (66.24 J/mol K) reflects the affinity of FABAC for MB dye.

Conclusion

Pc/CT composite ion exchanger was successfully prepared in an aqueous system under the ambient temperature and pH. Pc/CT composite was characterized by FTIR, SEM, TEM and XRD techniques. Pc/CT exhibited promising ion exchange capacity and thermal stability. pH titration curve confirmed the monofunctional nature of the composite material. The spectral analysis confirmed the formation of Pc/CT composite ion exchanger. Pc/CT was found most selective for Zn^{2+} separation in water system. Methylene dye was successfully removed using Pc/CT composite ion exchanger. Equilibrium data were fitted well in the Langmuir, Freundlich and Tempkin isotherms confirmed that the sorption is heterogeneous and occurred through physico-chemical interactions. The rate of sorption was found to obey pseudo-second-order kinetics and intraparticle diffusion model with a good correlation coefficient. The negative ΔG^0 values indicated that the sorption of dye onto biosorbent was feasible and spontaneous. The positive ΔH^0 value depicted endothermic nature of the sorption.

References

Abd EL, Latif MM, Ibrahim AM (2009) Adsorption, kinetic and equilibrium studies on removal of basic dye from aqueous solutions using hydrolyzed oa sawdust. Desalination Water Treat 6:252–268

Arrad O, Sasson Y (1989) Commercial ion exchange resins as catalysts in solid–solid–liquid reactions. J Org Chem 54: 4993–4998

Barka N, Qouzal S, Assabbane A, Nounhan A, Ichou YA (2011) Removal of reactive yellow 84 from aqueous solutions by adsorption ontohydroxyapaite. J Saudi Chem Soc 15:263–267

Bhattacharyya K, Sharma A (2005) Kinetics and thermodynamics of methylene blue adsorption on neem leaf powder. Dyes Pigment 66:51–59

Bushra R, Shahadat Md, Raeisssi AS, Nabi SA (2012) Development of nano-composite adsorbent for removal of heavy metals from industrial effluent and synthetic mixtures: its conducting behaviour. Desalination 289:1–11

Constantin M, Asmarandei I, Harabagiu V, Ghimici L, Ascenzi P, Fundueanu G (2013) Removal of anionic dyes from aqueous solutions by an ion-exchanger based on pullulan microsphere. Carbohydr Polym 91:74–84

Dogan M, Alkan M, Turkyilmaz A, Ozdemir Y (2004) Kinetics and mechanism of removal of methylene blue by adsorption onto perlite. J Hazard Mater B 109:141–148

Foo KY, Hameed BH (2012) Porous structure and adsorptive properties of pineapple peel based activated carbons prepared via microwave assisted KOH and K_2CO_3. Microporous Mesoporous Mater 148:191–195

Gupta VK, Jain R, Varshney S (2007) Electrochemical removal of the hazardous dye Reactofix Red 3 BFN from industrial effluents. J Colloid Interface Sci 312:292–296

Gupta VK, Mittal A, Malviya A, Mittal J (2009) Adsorption of carmoisine A from wastewater using waste materials-Bottom ash and deoiled soya. J Colloid Interface Sci 335:24–33

Gupta VK, Rastogi A, Nayak A (2010) Biosorption of nickel onto treated alga (Oedogoniumhatei): application of isotherm and kinetic models. J Colloid Interface Sci 342(2):533–539

Gupta VK, Agarwal S, Saleh TA (2011a) Chromium removal by combining the magnetic properties of iron oxide with adsorption properties of carbon nanotubes. Water Res 45:2207–2212

Gupta VK, Gupta B, Rastogi A, Nayak A, Agarwal S (2011b) A comparative investigation on adsorption performances of mesoporous activated carbon prepared from waste rubber tire and activated carbon for a hazardous azo dye-acid blue 113. J Hazard Mater 186:891–901

Gupta VK, Pathania D, Agarwal S, Singh P (2012) Preparation of cellulose acetate-zirconium (IV) phosphate nanocomposite with ion exchange capacity and enhanced photocatalytic activity. J Hazard Mater 243:179–186

Hassan SSM, Marei SA, Badr IH, Arida HA (2001) Novel solid-state ammonium ion potentiometric sensor based on zirconium titanium phosphate ion exchanger. Anal Chim Acta 427:21–28

Huang SH, Chen DH (2009) Rapid removal of heavy metals cations and anions from aqueous solution by an amino-functionalized magnetic nano-adsorbent. J Hazard Mater 163:174–179

Ibrahim S, Shuy WZ, Ang HM, Wang S (2010) Preparation of bioadsorbents for effective adsorption of a reactive dye in aqueous solution. Chem Eng J 5:563–569

Islam M, Patel R (2008) Polyacrylamide thorium (IV) phosphate as an important lead selective fibrous ion exchanger: synthesis, characterization and removal study. J Hazard Mater 156: 509–520

Khan AA, Khan A (2010) Ion-exchange studies on poly-o-anisidine Sn(IV) phosphate nanocomposite and its application as Cd(II) ion-selective membrane electrode. Eur J Chem 8(2):396–408

Khan AA, Paquiza L (2011) Analysis of mercury ions in effluents using potentiometric sensor based on nanocomposite cation exchanger polyaniline-zirconium titanium phosphate. Desalination 272:278–285

Kumar KV, Kumaran A (2005) Removal of methylene blue by mango seed kernel powder. Biochem Eng J 27:83–93

Langmuir I (1916) The constitution and fundamental properties of solids and liquids. J Am Chem Soc 38:2221–2295

Liang S, Guo X, Feng N, Tian Q (2010) Isotherms, kinetics and thermodynamic studies of adsorption of Cu2 + from aqueous solutions by Mg2 +/K + type orange peel adsorbent. J Hazard Mater 174:756–762

Liu Y, Liu YJ (2008) Biosorption isotherms, kinetics and thermodynamics. Sep Purif Technol 61:229–242

Malik PK (2004) Dye removal from wastewater using activated carbon developed from sawdust: adsorption equilibrium and kinetics. J Hazard Mater B 113:81–88

Miller FA, Wilkins CH (1952) Infrared spectra and characteristic frequencies of inorganic ions. Anal Chem 24:1253–1294

Nabi SA, Naushad Mu (2008) Synthesis, characterization and analytical applications of a new composites cations exchanger cellulose acetate—Zr (IV) molybdophosphate. Colloids Surf A Phys Eng Aspects 316:217–225

Nabi SA, Shahadat Md, Bushra R, Shalla AH, Ahmed F (2010) Development of composite ion-exchange adsorbents for pollutant removal from environmental waste. Chem Eng J 165:405–412

Nabi SA, Shahadat Md, Bushra R, Shalla AH, Azam A (2011) Synthesis and characterization of nano-composite ion-exchanger: its adsorption behaviour. Colloids Surf B Bio 87:122–128

Nemr AE, Abdel WO, Amany ES, Khaled A (2009) Removal of direct blue-86 from aqueous solution by new activated carbon developed from orange peel. J Hazard Mater 161:102–110

Pathania D, Sharma S (2012) Effect of surfactants and electrolyte on removal and recovery of basic dye by using *Ficus carica* cellulosic fibers as biosorbent. Tenside Surf Deter 2012(04): 306–314

Shi L, Gunasekaran S (2008) Preparation of pectin-ZnO nanocomposite. Nanoscale Res Lett 3:491–495

Siddiqi ZM, Pathania D (2003) Studies on Ti(VI) tungstosilicate and Ti(VI) tungstophosphate: two new inorganic ion exchangers. J Chromatrogr J 987:147–158

Siddiqui WA, Khan SA, Inamuddin (2007) Synthesis, characterization and ion-exchange properties of a new and novel 'organic–inorganic hybrid' cation-exchanger: poly(methylenemethacrylate) Zr (IV) phosphate. Coll Surf A Phys Eng Aspects 295:193–199

Vatutsina OM, Soldatov VS, Sokolova VI, Johann J, Bissen M, Weisswnbacher A (2007) A new hybrid (polymer/inorganic) fibrous sorbents for arsenic removal from drinking water. Funct Polym 67:184–201

Wang XS, Qin Y (2005) Equilibrium sorption isotherms for of Cu2 + on rice bran. Process Biochem 40:677–680

Yang Z, Chen S, Hu W, Yin N, Zhang W, Xiang C, Wang H (2012) Flexible luminescent CdSe/bacterial cellulose nanocomposite membrane. Carbohydr Polym 88:173–178

2024

Int. J. Environ. Sci. Technol. (2014) 11:2015–2024

Zacar MO, Engil IAS (2004) Application of kinetic models to the sorption of disperse dyes onto alunite. Colloids Surf Physicochem 42:105–113

Zhao X-T, Zeng T, Hu ZJ, Gao H-W, Zou CY (2012a) Modeling and mechanism of the adsorption of proton onto natural bamboo sawdust. Carbohydr Polym 87:1199–1205

Zhao X-T, Zeng T, Li X-Y, Hu ZJ, Gao H-W, Xie Z (2012b) Modeling and mechanism of the adsorption of copper ion onto natural bamboo sawdust. Carbohydr Polym 89:85–192